Title

Effect of mitral annuloplasty device shape and size on leaflet and myofiber stress following repair of posterior leaflet prolapse: a patient-specific finite element simulation.

Journal

The Journal of Heart Valve Disease, 23(6)

ISSN

0966-8519

Authors

Morrel, William G
Ge, Liang
Zhang, Zhihong
et al.

Publication Date

2014-11-01

Peer reviewed

HHS Public Access

Author manuscript

J Heart Valve Dis. Author manuscript; available in PMC 2018 July 11.

Published in final edited form as:

J Heart Valve Dis. 2014 November ; 23(6): 727–734.

Effect of mitral annuloplasty device shape and size on leaflet and myofiber stress following repair of posterior leaflet prolapse: A patient-specific finite element simulation

William G. Morrel, BS[1], **Liang Ge, PhD**[2,4], **Alison Ward**[5], **Zhihong Zhang, MS**[4], **Eugene A. Grossi**[5], **Julius M. Guccione, PhD**[1,2,4], and **Mark B. Ratcliffe, MD**[2,3,4]

[1]School of Medicine, University of California, San Francisco, California

[2]Department of Surgery, University of California, San Francisco, California

[3]Department of Bioengineering, University of California, San Francisco, California

[4]Veterans Affairs Medical Center, San Francisco, California

[5]Department of Cardiothoracic Surgery, New York University

Abstract

Background—Mitral annuloplasty (MA) devices have different shapes and sizes. However, the preferred shape and size are unclear.

Methods—A previously described and validated finite element (FE) model of the left ventricle (LV) with mitral valve (MV) based on MRI and 3D echo images from a patient with posterior leaflet (PL; P2) prolapse was used. FE models of MA devices with different shapes (flat partial, shallow saddle, pronounced saddle) and sizes (36–30) were created. Virtual leaflet resection + MA with each shape and size were simulated. Leaflet geometry, stresses in the leaflets and base of the LV, and forces in the chordae and MA sutures were calculated.

Results—All MA shapes increased mitral coaptation length, reduced the elevated PL stress at end-diastole (ED) and end-systole (ES) that occurred after leaflet resection, and reduced anterior leaflet (AL) stress at ES. Reduction in MA size for each MA shape further decreased PL stress at ED and ES and AL stress at ES. MA devices of all shapes and sizes modestly reduced myofiber stress at the LV base in ED and ES. In general, saddle-shaped devices had the greatest effect.

Conclusions—All MA shapes increased coaptation length and reduced mitral leaflet stress and myofiber stress in the base of the LV. Additional reduction in MA size further increased coaptation length and reduced leaflet and myofiber stress. In general, saddle-shaped devices had the greatest effect.

Keywords

Mitral prolapse; Mitral regurgitation; Finite element; Annuloplasty

Corresponding Author: Mark B. Ratcliffe, MD, Division of Surgical Services (112), San Francisco Veterans Affairs Medical Center, 4150 Clement Street, San Francisco, California 94121. Telephone: (415) 221-4810. FAX: (415) 750-2181. Mark.Ratcliffe@va.gov.

Disclosure: Dr. Grossi receives royalties from Medtronic for annuloplasty devices and receives consulting fees and royalties from Edwards Life Sciences.

Introduction

A common mitral valve (MV) repair for mitral prolapse is leaflet resection combined with mitral annuloplasty (MA). MV repair for severe mitral regurgitation (MR) is indicated in patients with symptoms, patients with systolic dysfunction, and asymptomatic patients in whom repair is likely to succeed. (1) Operative mortality and initial correction of MR are excellent after MV repair for degenerative disease. The addition of an annuloplasty device strongly enhances repair durability. (2)

On the other hand, recurrent 2–4+ MR after MV repair may occur at a rate of 2.6% per year even after exclusion of patients with Barlow's syndrome. (3) Freedom from reoperation progresses more slowly but can reach 20% at 19.5 years. (4) Results from low volume centers are probably worse.

One significant problem is that mitral repair techniques are not standardized. (5) For instance, a variety of MA devices are available, many of which are designed to recreate the normal valve saddle shape (6, 7) while others opt for a flat shape. (8) Stiffness ranges from flexible to semi-rigid to stiff, and in each case a range of sizes is available. (5) Repair durability and the low likelihood of mitral repair in this country (41–69% (9, 10)) may be partially due to this lack of standardization and experience with significantly low individual surgeon/center volume.

To the best of our knowledge, only our lab has developed finite element (FE) models of the left ventricle (LV) and MV. (11, 12) With those models, we have studied MA device shape in the setting of ischemic mitral regurgitation. (11) Most recently, we built a patient-specific finite element model of the human LV + MV with posterior leaflet (PL; P2) prolapse type degenerative MR. Finally, we performed virtual MV repair surgery to mimic the surgery the patient received and showed that it matched patient data on several key metrics. (13)

In the present study, we used our validated FE model of the LV + MV with P2 prolapse to calculate the effect of annuloplasty device shape and size on leaflet stress and myofiber stress in the LV. We tested the hypothesis that a saddle-shaped annuloplasty device is best able to increase leaflet coaptation and reduce leaflet and LV myofiber stresses and that reduction in annuloplasty device size is associated with further improvement in coaptation and reduction in stress.

Methods

FE model of mitral valve repair

Overview—Briefly, a finite element mesh including LV, mitral valve, and chordae tendineae based on pre and intra-operative imaging data from a patient with posterior leaflet prolapse was created as previously described. (14) The diastolic and systolic material parameters of the LV in the pre-repair model were manually adjusted so that the model's LV volumes at end-diastole (ED) and end-systole (ES) were within 5% of LV volumes measured with MRI. (14) Virtual triangular resection of the P2 region of the posterior leaflet and MA

were sequentially performed using the virtual suture method as previously described. (11, 14) Resection was modeled on videoscopic recording of the actual operation.

Virtual annuloplasty—Flat partial, shallow saddle, and pronounced saddle shaped MA devices were digitized by scanning physical samples using microCT (Scanco μCT 50). Device shapes are shown in Figure 1 and properties are summarized in Table 1. The exterior fabric portion of the devices was excluded from the FE model. Contours were created to represent the devices in three dimensions using Rapidform XOR2 SP1 (3D Systems, Rock Hill, SC, USA). A mesh of each device was created using beam elements. The devices were assumed to be rigid in our simulation (*MAT_RIGID, LS-DYNA, Livermore, CA). MA device meshes were scaled to match the diameters of the 2 MA devices produced by Medtronic (Table 2). For instance, all size 36 MA device meshes had a transverse diameter of 38.45 mm.

Each annuloplasty device mesh was placed near the center of the mitral valve. Virtual sutures were added to pull the mitral annulus towards the annuloplasty device as previously described. (11) Simulation of LV diastole and systole then proceeded as previously described. (12)

Measurement of leaflet geometry—Overlap of the anterior and posterior mitral leaflets (coaptation length) was calculated from each FE model. Leaflets were considered to be overlapping if the distance between them in the FE model results was less than 1.5 mm. Slices were taken every 1.43 mm.

Stress and force calculations—The LV was divided equally into basal, middle, and apical regions. Mitral leaflets were each divided into A1 (left anterior), A2, and A3, and P1 (left posterior), P2, and P3 scallops. LV fiber stress, mitral leaflet von Mises (effective) stress, and uniaxial forces in the virtual sutures were calculated. Strain was computed with ED as the reference configuration.

Statistical analysis—Stress and strain were averaged over all elements of each LV or leaflet region and presented as the average ± the standard deviation in each region. The FE model was based on a single patient. The results obtained are not stochastic and statistical tests were therefore not appropriate. P values are therefore not reported.

Results

Leaflet geometry

The effects of annuloplasty device shape and size on coaptation length at end-systole are seen in Figure 2. All shapes increased leaflet coaptation length. Also, within each shape, a reduction in device size was associated with an increase in coaptation length. The pronounced saddle shape device was associated with the greatest increase in coaptation length and the greatest increase in coaptation length with size reduction. For instance, peak coaptation length in the P3 region increases from 5.4 mm pre-op (Figure 2A) to 11.3 mm with a size 36 pronounced saddle MA device and to 14.3 mm with a size 30 (Figure 2D).

Leaflet stress

All MA shapes reduced the elevated stress in the posterior leaflet that occurred after triangular resection of the posterior leaflet (Figures 3A and B). Also, within each shape, a reduction in device size was associated with a further reduction in stress such that posterior leaflet stress at end-systole was lower than pre-op after application of both flat and saddle-shaped 30 mm devices (Figure 3C). Finally, the pronounced saddle shape was associated with the greatest reduction in end-systolic stress in the posterior leaflet although the difference between pronounced saddle and the other devices was small.

The effect of MA shape and size on stress in the anterior leaflet was more complex. First, triangular resection of the posterior leaflet reduces stress in the anterior leaflet (Figures 3B and D) rather than increasing stress as seen in the posterior leaflet. Compared to end-diastolic stress after resection, the effect of MA shape on anterior leaflet stress at end-diastole was variable: the flat band caused a reduction, the shallow saddle had little effect, and the pronounced saddle actually increased stress (Figure 3B). Further, MA size had minimal effect. It should be noted that this pattern is similar to the pattern seen when measuring forces in the chordae that attach to the anterior leaflet at end-diastole.

When compared to stress after resection, all MA shapes were associated with further reduction in anterior leaflet stress at end-systole (Figure 3D). Similar to the posterior leaflet, smaller device size was associated with further stress reduction, and the shallow and pronounced saddle shapes caused the greatest stress reduction. For instance, anterior leaflet stress at end-systole with the 30 mm flat band was 55.5 kPa but 43.1 with the shallow saddle (22% reduction).

Chordal force

The pattern in chordal force at end-diastole (Figures 4A and B) is similar to leaflet stress at end-diastole with saddle-shaped devices having the greatest reduction in the posterior leaflet but the greatest increase in force in the chords to the anterior leaflet.

With regard to chordal force at end-systole, the saddle-shaped devices were associated with the lowest chordal force to both the anterior and posterior leaflets (Figures 4C and D). The size of the flat band had no effect on anterior leaflet chordal force at end-systole (Figure 4D). With that exception, within each group, a reduction in MA size was associated with a reduction in chordal force to both the anterior and posterior leaflets.

Myofiber stress

At end-diastole, the flat band and shallow saddle led to relatively unchanged myofiber stress in the basal region of the LV (98.7% and 100.5% of baseline, respectively), while the pronounced saddle reduced myofiber stress to 60.3% of baseline (Figure 5A). At end-systole, saddle-shaped devices led to lower myofiber stress: flat band, shallow saddle, and pronounced saddle reduced stress to 88.4%, 80.3%, and 80.9% of baseline, respectively (Figure 5B).

With regard to device size, myofiber stress in the basal region of the LV at end-diastole was lowest at device size 30 for the flat band and shallow saddle but at size 36 for the

pronounced saddle (Figure 5A). At end-systole, myofiber stress decreased consistently with decreasing device size for the flat band. For saddle-shaped devices, myofiber stress increased slightly from size 36 to size 34 and then steadily decreased as device size decreased. (Figure 5B)

Suture force

Figure 6 shows the average suture force at end-diastole (**A**) and end-systole (**B**). At both end-diastole and end-systole, the saddle-shaped devices were associated with the greatest force on sutures with the shallow saddle having the highest forces. With the flat band, reduction in size from 36 to 30 had little effect on suture force (ED: 1.19 N to 1.22 N; ES: 1.63 N to 1.75 N), but with saddle-shaped devices size reduction led to an increase in suture force at end-diastole and end-systole (ED: 2.12 N to 2.37 N for shallow saddle and 1.67 N to 2.02 N for pronounced saddle; ES: 2.43 N to 2.98 N for shallow saddle and 2.12 N to 2.46 N for pronounced saddle).

Discussion

The principal findings of the study are that 1) all MA shapes increased coaptation length and reduced mitral leaflet stress and myofiber stress in the base of the LV, 2) reduction in MA size further increased coaptation length and reduced leaflet and myofiber stress, and 3) saddle-shaped devices had the greatest effect.

Leaflet geometry and coaptation

Flattening of the normal saddle shape of the mitral annulus (15) occurs in patients with mitral valve prolapse and is associated with the development of significant MR. (16) Our findings support the hypothesis that recreation of the annular saddle shape in patients with mitral valve prolapse is best able to increase leaflet coaptation and reduce leaflet and LV myofiber stresses. With regard to leaflet coaptation, our findings are in agreement with a previous study by Vergnat et al. [8] who studied patients with posterior leaflet prolapse and found that post-operative leaflet coaptation area was significantly greater in those that received a saddle-shaped annuloplasty device.

Our findings also support the hypothesis that reduction in annuloplasty device size is associated with further improvement in coaptation and reduction in stress. In that regard, the only data that we are aware of relating annuloplasty size with coaptation comes from the experience with adjustable annuloplasty devices. (17) Maisano and colleagues implanted semi-rigid adjustable MA devices in patients with severe MR. Reduction of the posterior annulus perimeter was associated with an increase in coaptation length of 3 mm. (17) Our data are in general agreement where a change in device size from 36 to 30 in each device shape was associated with an increase in coaptation length between 2 and 4 mm.

Leaflet stress

The second area of benefit associated with recreation of the annular saddle shape is leaflet stress reduction. Specifically, our findings are in agreement with a previous study by Salgo et al. who used FE models of the mitral valve based on idealized leaflet geometry to show

that saddle shape (increase in the annular height to commissural width ratio) was associated with an increase in leaflet radius of curvature and a decrease in leaflet stress. (18) Also, in a study of patients with ischemic MR, Vergnat et al. (7) found that patients who received a saddle-shaped device had significantly greater leaflet curvature, an indirect measure of stress, in all leaflet regions compared with patients who received a flat device.

We also found that reduction in annuloplasty device size reduces stress in both leaflets at end-systole versus a true-sized device (size 36 in this model). Regardless of shape, a device undersized by 2–3 sizes decreased myofiber stress at end-systole. At end-diastole, undersizing decreased myofiber stress for the flat band and shallow saddle but increased myofiber stress for the pronounced saddle. To our knowledge, our study is the only one to look at the effect of annuloplasty size.

Our study simulated annuloplasty in conjunction with triangular resection of the posterior leaflet and the end effect on leaflet stress must be seen in relation to the effect of leaflet resection, which significantly increases stress in the posterior leaflet and decreases stress in the anterior leaflet. It is probable that other types of leaflet resection and plasty will have similar effects although of different magnitude. The addition of neochords is expected to reduce stress in the posterior leaflet but further work in this area is needed.

Chordal force

The one instance in which re-creation of the saddle-shaped annulus increased leaflet stress is in the anterior leaflet at end-diastole. The fact that force on the chords to the anterior leaflet at end-diastole is also increased with a saddle-shaped device suggests that the etiology is atrial displacement of the anterior annulus by the saddle-shaped device, effectively stretching the anterior leaflet and chords to the anterior leaflet between the device and the papillary muscles.

Our findings are at odds with those of Jimenez et al. who measured chordal force *in vitro* in human mitral valves mounted in the left heart simulator and found that a saddle-shaped annulus was associated with reduction in anterior strut chord tension but an increase in tension in the posterior intermediate and commissural chords. (19) We suspect the difference between our findings and those of Jimenez is due to the valve mounting method employed by Jimenez in which the anterior section of the annulus was fixed in place. Our method, on the other hand, allows the annulus to deform according to material properties of the annulus and base of the heart. Further experimental studies are warranted.

Basal myofiber stress

The pronounced saddle achieved the greatest reduction in end-diastolic myofiber stress (60.3% of baseline). End-systolic myofiber stress was minimized with the shallow saddle (80.3% of baseline) but the pronounced saddle achieved similar results (80.9% of baseline). Given the high end-diastolic myofiber stress with the shallow saddle (100.5% of baseline), the pronounced saddle achieved the best overall myofiber stress profile.

Force on annuloplasty sutures

We found that forces on sutures that approximate the annulus to the annuloplasty device are greatest in the saddle-shaped devices. We also found that reduction in annuloplasty device size causes suture force to increase. Annuloplasty suture force has not been experimentally measured in animals or in humans. However, our findings are consistent with those of Jensen et al. who implanted flat and saddle-shaped annuloplasty devices instrumented with load cells in normal pigs and found that saddle-shaped devices were associated with decreased force perpendicular to the valve plane. (20) This is significant because high suture force is a surrogate for valve dehiscence.

Limitations

The study was based on a single patient and a follow-up study using multiple patient-specific FE models is indicated.

There is a tradeoff between MA device size and resistance to flow across the valve especially during exercise. For instance Mesana et al. found significant late elevation in mitral valve gradient and pulmonary pressure in patients who received either partial (average size 30.7 + 2.8) or complete (average size 30.4 + 2.1) annuloplasty devices for posterior leaflet prolapse. (21) Calculation of the gradient across the mitral valve in our models with computational flow dynamic methods is possible but beyond the scope of this study.

In order to isolate the effect of shape, the actually stiffness of the MA devices was ignored as was shape change. A follow-up study analyzing the effect of device stiffness would provide further insight into the optimal design for minimizing myofiber and leaflet stress. Because this study did not take device stiffness into account, it is not possible to conclude that one model of device is preferred over another, only that one shape or size may be preferred. Indeed, a semi-rigid device allows changes in the valvular orifice during the cardiac cycle, which may be beneficial with respect to post repair gradients. (22) This information may be useful for informing future MA device design, however.

This study assumed that device shape remained consistent as size was varied. In reality, this is not true as some devices (e.g. Physio II) have a more pronounced curvature at larger sizes. The sizes of the actual physical devices used to create the FE representations are listed in Table 2.

Last, there is a need for more and better leaflet material property data obtained either by inverse calculation of leaflet properties (probably by comparison with echo-measured shape) or by direct measurement of leaflet tissue stiffness obtained in the operating room on the biaxial stretcher. Barber and colleagues found that valve tissue from patients with myxomatous mitral valve disease is stiffer than normal during uniaxial stretching. (23) However, uniaxial stretching is generally thought to be indeterminate and further studies using a biaxial testing apparatus are warranted.

Conclusion and Future Directions

The principal findings of the study are that 1) all MA shapes reduced mitral leaflet stress, 2) reduction in MA size increased the stress reduction, and 3) saddle-shaped devices had the greatest effect. Last, the FE method is able to quantitate the effect of MA shape and size on leaflet and myofiber stress.

Creation of FE models based on additional patients is on-going. Furthermore, future models could incorporate device stiffness and fluid-structure interaction. Also, material properties of the MV could be measured using a tissue stretcher and incorporated into the model to more accurately simulate MV movement. Finally, this method has the potential to calculate optimal MA device shape (beyond currently available designs) and to create a virtual training tool for surgical trainees.

Acknowledgments

This study was supported by NIH grants R01-HL-63348 (Dr. Ratcliffe) and R01-HL-077921 (Dr. Guccione) and by AHA grant 13MSRF17090108. This support is gratefully acknowledged.

References

1. Foster E. Clinical practice. Mitral regurgitation due to degenerative mitral-valve disease. N Engl J Med. 2010 Jul 8; 363(2):156–65. PubMed PMID: 20647211. Epub 2010/07/22. eng. [PubMed: 20647211]
2. Gillinov AM, Tantiwongkosri K, Blackstone EH, Houghtaling PL, Nowicki ER, Sabik JF 3rd, et al. Is prosthetic anuloplasty necessary for durable mitral valve repair? Ann Thorac Surg. 2009 Jul; 88(1):76–82. PubMed PMID: 19559197. [PubMed: 19559197]
3. Flameng W, Meuris B, Herijgers P, Herregods MC. Durability of mitral valve repair in Barlow disease versus fibroelastic deficiency. J Thorac Cardiovasc Surg. 2008 Feb; 135(2):274–82. PubMed PMID: 18242250. Epub 2008/02/05. eng. [PubMed: 18242250]
4. Mohty D, Orszulak TA, Schaff HV, Avierinos JF, Tajik JA, Enriquez-Sarano M. Very long-term survival and durability of mitral valve repair for mitral valve prolapse. Circulation. 2001 Sep 18; 104(12 Suppl 1):I1–I7. PubMed PMID: 11568020. Epub 2001/09/25. eng. [PubMed: 11568020]
5. Bothe W, Miller DC, Doenst T. Sizing for mitral annuloplasty: where does science stop and voodoo begin? Ann Thorac Surg. 2013 Apr; 95(4):1475–83. PubMed PMID: 23481703. [PubMed: 23481703]
6. Vohra HA, Whistance RN, Bezuska L, Livesey SA. Initial experience of mitral valve repair using the Carpentier-Edwards Physio II annuloplasty ring. Eur J Cardiothorac Surg. 2011 Jun; 39(6):881–5. PubMed PMID: 21106384. [PubMed: 21106384]
7. Vergnat M, Levack MM, Jassar AS, Jackson BM, Acker MA, Woo YJ, et al. The influence of saddle-shaped annuloplasty on leaflet curvature in patients with ischaemic mitral regurgitation. Eur J Cardiothorac Surg. 2012 Sep; 42(3):493–9. PubMed PMID: 22351705. Pubmed Central PMCID: 3417051. [PubMed: 22351705]
8. Fasol R, Meinhart J, Deutsch M, Binder T. Mitral valve repair with the Colvin-Galloway Future Band. Ann Thorac Surg. 2004 Jun; 77(6):1985–8. discussion 8. PubMed PMID: 15172250. [PubMed: 15172250]
9. Bolling SF, Li S, O'Brien SM, Brennan JM, Prager RL, Gammie JS. Predictors of mitral valve repair: clinical and surgeon factors. Ann Thorac Surg. 2010 Dec; 90(6):1904–11. discussion 12. PubMed PMID: 21095334. Epub 2010/11/26. eng. [PubMed: 21095334]
10. Gammie JS, Sheng S, Griffith BP, Peterson ED, Rankin JS, O'Brien SM, et al. Trends in mitral valve surgery in the United States: results from the Society of Thoracic Surgeons Adult Cardiac

Surgery Database. Ann Thorac Surg. 2009 May; 87(5):1431–7. discussion 7–9. PubMed PMID: 19379881. Epub 2009/04/22. eng. [PubMed: 19379881]

11. Wong VM, Wenk JF, Zhang Z, Cheng G, Acevedo-Bolton G, Burger M, et al. The effect of mitral annuloplasty shape in ischemic mitral regurgitation: a finite element simulation. Ann Thorac Surg. 2012 Mar; 93(3):776–82. PubMed PMID: 22245588. Pubmed Central PMCID: 3432639. Epub 2012/01/17. eng. [PubMed: 22245588]
12. Wenk JF, Zhang Z, Cheng G, Malhotra D, Acevedo-Bolton G, Burger M, et al. First finite element model of the left ventricle with mitral valve: insights into ischemic mitral regurgitation. Ann Thorac Surg. 2010 May; 89(5):1546–53. PubMed PMID: 20417775. Epub 2010/04/27. eng. [PubMed: 20417775]
13. Ge L, Morrel WG, Ward A, Mishra R, Zhang Z, Guccione JM, et al. Measurement of mitral leaflet and annular geometry and stress after repair of posterior leaflet prolapse: virtual repair using a patient-specific finite element simulation. Ann Thorac Surg. 2014 May; 97(5):1496–503. PubMed PMID: 24630767. Pubmed Central PMCID: 4121378. [PubMed: 24630767]
14. Ge L, Morrel WG, Ward A, Mishra R, Zhang Z, Guccione JM, et al. Measurement of Mitral Leaflet and Annular Geometry and Stress After Repair of Posterior Leaflet Prolapse: Virtual Repair Using a Patient-Specific Finite Element Simulation. Ann Thorac Surg. 2014 Mar 12. PubMed PMID: 24630767.
15. Levine RA, Handschumacher MD, Sanfilippo AJ, Hagege AA, Harrigan P, Marshall JE, et al. Three-dimensional echocardiographic reconstruction of the mitral valve, with implications for the diagnosis of mitral valve prolapse. Circulation. 1989 Sep; 80(3):589–98. PubMed PMID: 2766511. Epub 1989/09/01. eng. [PubMed: 2766511]
16. Lee AP, Hsiung MC, Salgo IS, Fang F, Xie JM, Zhang YC, et al. Quantitative analysis of mitral valve morphology in mitral valve prolapse with real-time 3-dimensional echocardiography: importance of annular saddle shape in the pathogenesis of mitral regurgitation. Circulation. 2013 Feb 19; 127(7):832–41. PubMed PMID: 23266859. [PubMed: 23266859]
17. Maisano F, Falk V, Borger MA, Vanermen H, Alfieri O, Seeburger J, et al. Improving mitral valve coaptation with adjustable rings: outcomes from a European multicentre feasibility study with a new-generation adjustable annuloplasty ring system. Eur J Cardiothorac Surg. 2013 Nov; 44(5): 913–8. PubMed PMID: 23530026. [PubMed: 23530026]
18. Salgo IS, Gorman JH 3rd, Gorman RC, Jackson BM, Bowen FW, Plappert T, et al. Effect of annular shape on leaflet curvature in reducing mitral leaflet stress. Circulation. 2002 Aug 6; 106(6):711–7. PubMed PMID: 12163432. [PubMed: 12163432]
19. Jimenez JH, Soerensen DD, He Z, He S, Yoganathan AP. Effects of a saddle shaped annulus on mitral valve function and chordal force distribution: an in vitro study. Ann Biomed Eng. 2003 Nov; 31(10):1171–81. PubMed PMID: 14649491. Epub 2003/12/03. eng. [PubMed: 14649491]
20. Jensen MO, Jensen H, Smerup M, Levine RA, Yoganathan AP, Nygaard H, et al. Saddle-shaped mitral valve annuloplasty rings experience lower forces compared with flat rings. Circulation. 2008 Sep 30; 118(14 Suppl):S250–5. PubMed PMID: 18824763. Epub 2008/10/10. eng. [PubMed: 18824763]
21. Mesana TG, Lam BK, Chan V, Chen K, Ruel M, Chan K. Clinical evaluation of functional mitral stenosis after mitral valve repair for degenerative disease: potential affect on surgical strategy. J Thorac Cardiovasc Surg. 2013 Dec; 146(6):1418–23. discussion 23-5. PubMed PMID: 24075470. [PubMed: 24075470]
22. Sharony R, Saunders PC, Nayar A, McAleer E, Galloway AC, Delianides J, et al. Semirigid partial annuloplasty band allows dynamic mitral annular motion and minimizes valvular gradients: an echocardiographic study. Ann Thorac Surg. 2004 Feb; 77(2):518–22. discussion 22. PubMed PMID: 14759429. [PubMed: 14759429]
23. Barber JE, Kasper FK, Ratliff NB, Cosgrove DM, Griffin BP, Vesely I. Mechanical properties of myxomatous mitral valves. J Thorac Cardiovasc Surg. 2001 Nov; 122(5):955–62. PubMed PMID: 11689801. [PubMed: 11689801]

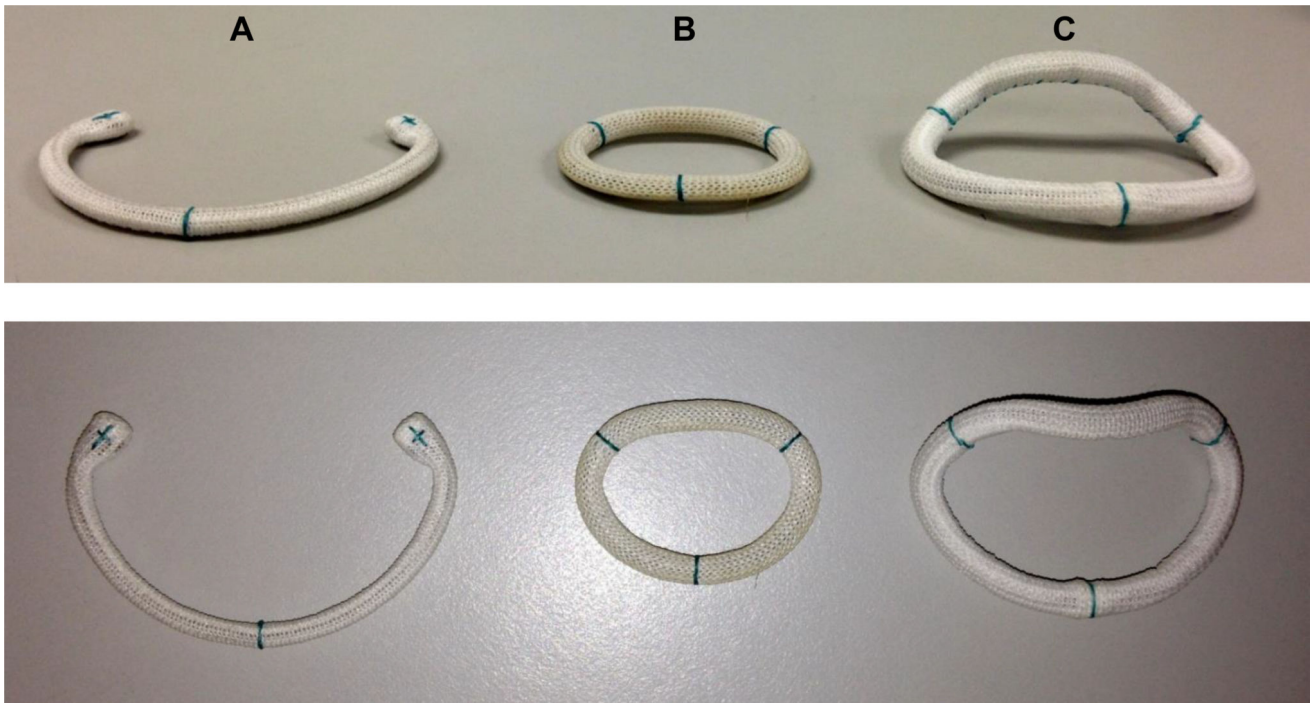

Figure 1.
Comparison of the three annuloplasty devices analyzed: **A)** flat band, **B)** shallow saddle and, **C)** pronounced saddle

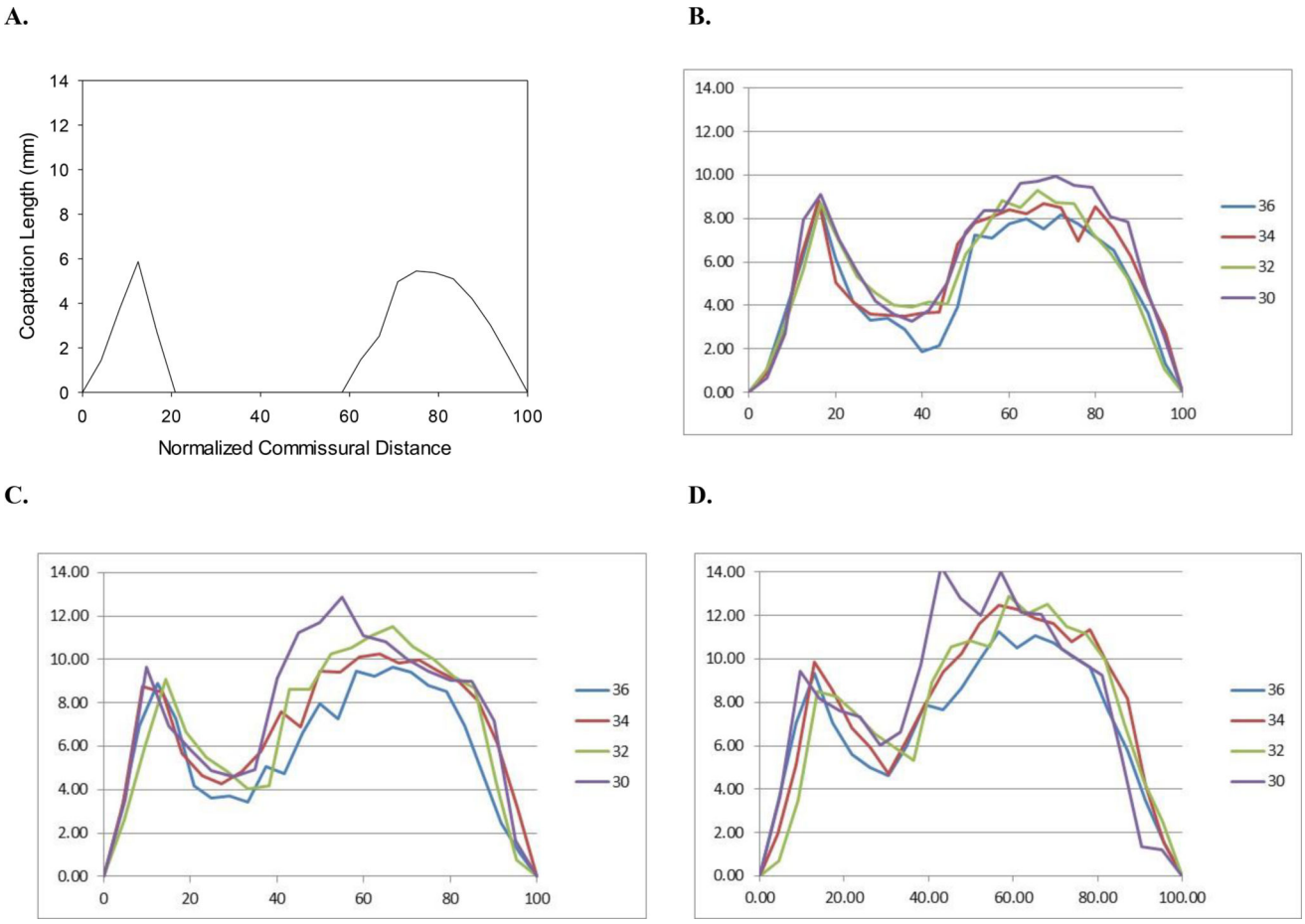

Figure 2.

Coaptation length at end-systole for **A)** Pre-operative, **B)** flat band, **C)** shallow saddle, and **D)** pronounced saddle. Normalized coaptation length is shown on the X axis extending from the left (0) to the right (100) commissure.

A.

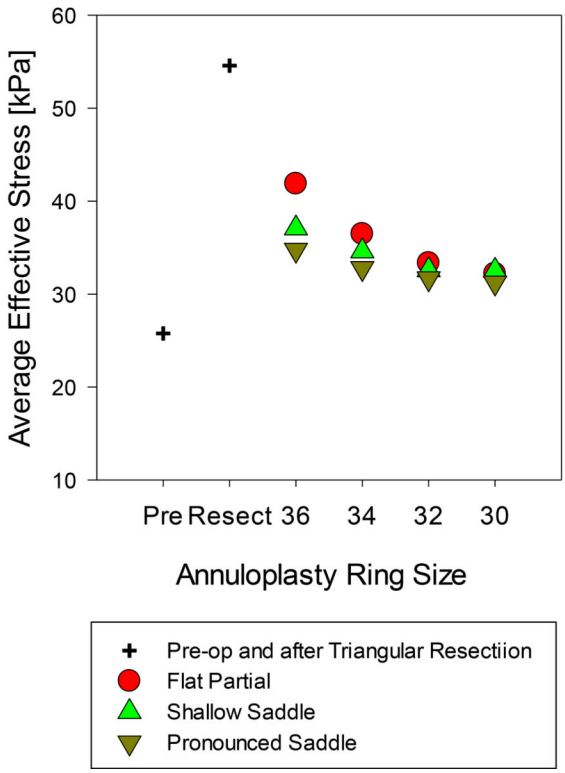

B.

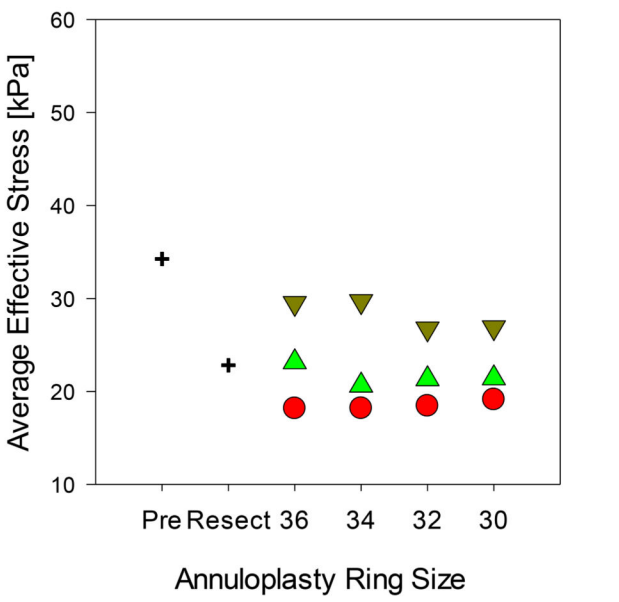

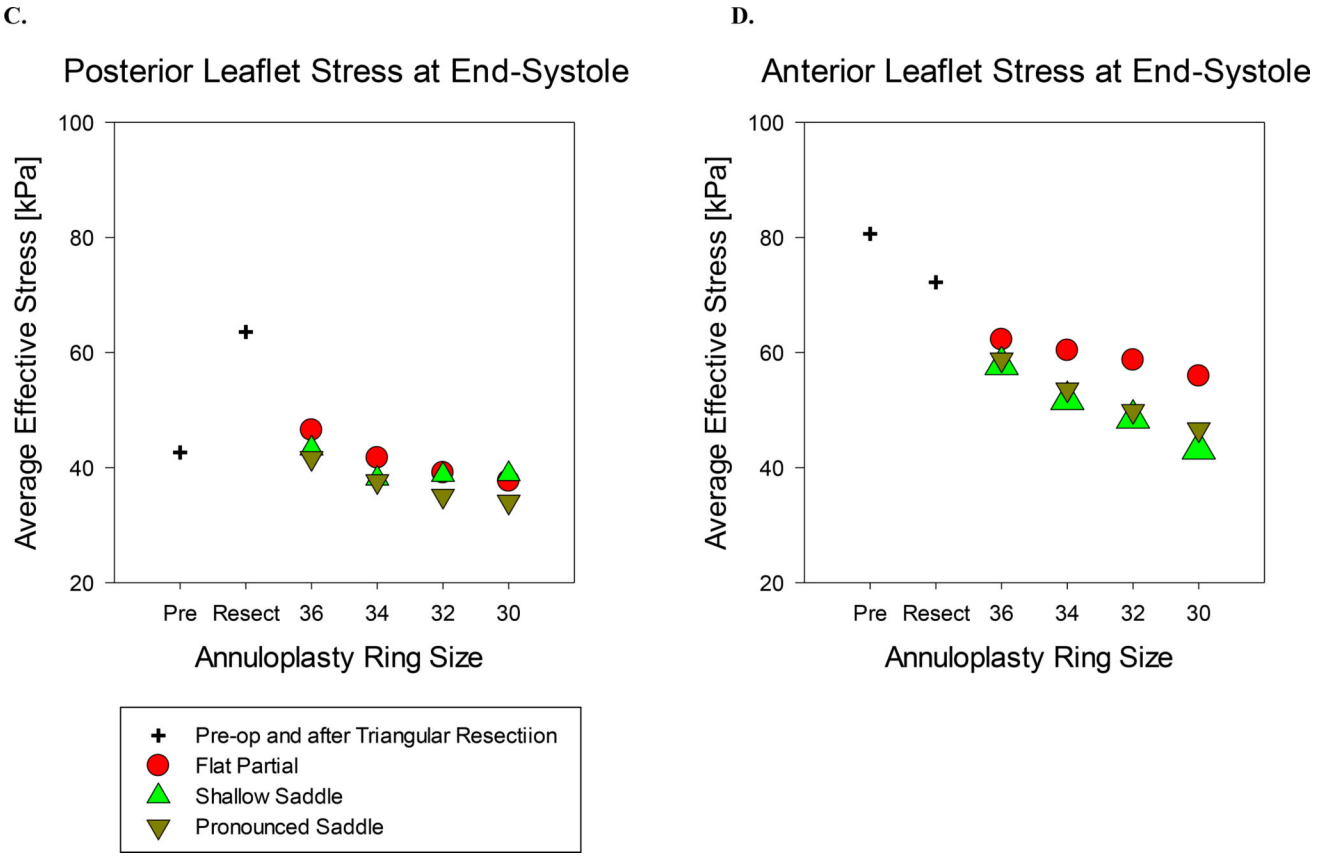

Figure 3.

Average von Mises leaflet stress at end-diastole in the posterior (**A**) and anterior (**B**) leaflets. Average leaflet stress at end-systole in the posterior (**C**) and anterior (**D**) leaflets. “Pre” refers to the pre-operative model. “Resect” refers to a model in which triangular leaflet resection was performed prior to mitral annuloplasty. 30, 32, 34 and 36 are annuloplasty device sizes.

A.

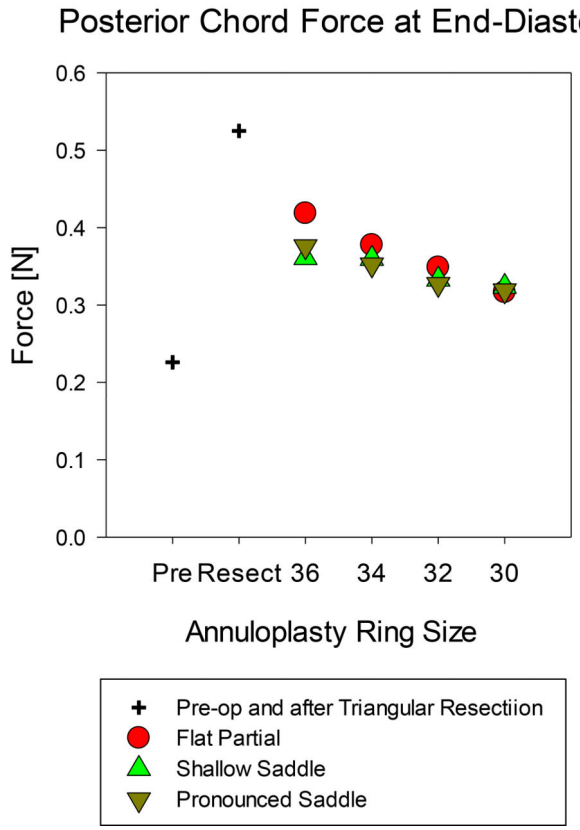

B.

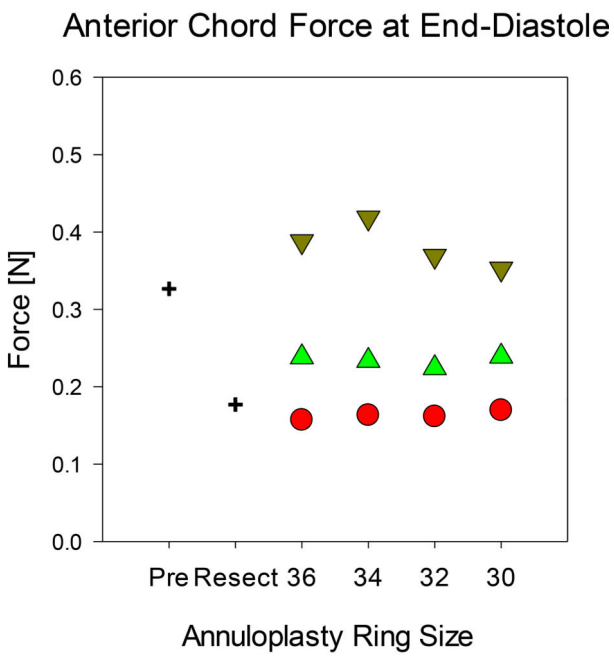

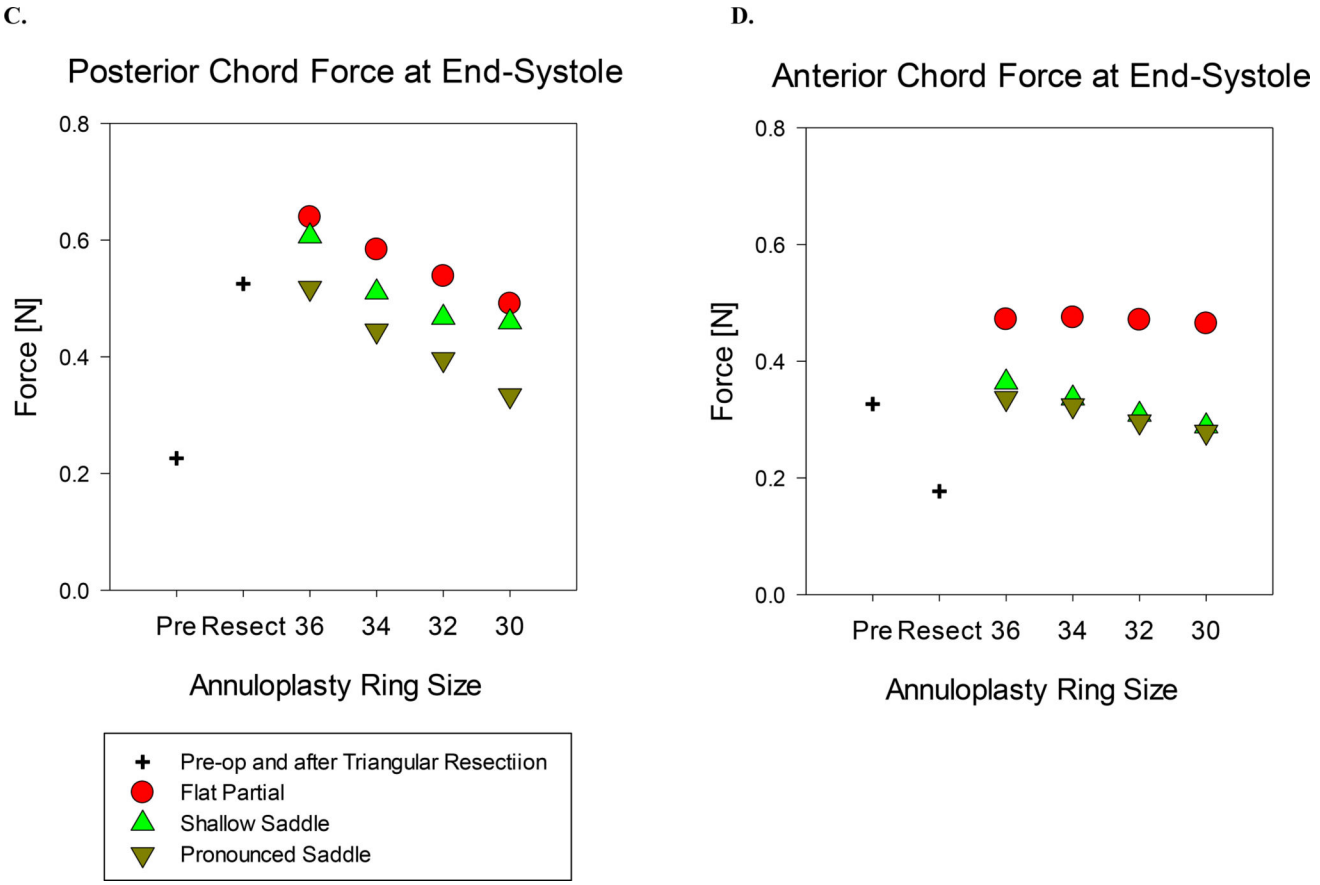

Figure 4.

Chordal force at end-diastole in the posterior (**A**) and anterior (**B**) leaflets. Abbreviations are similar to Figure 2.

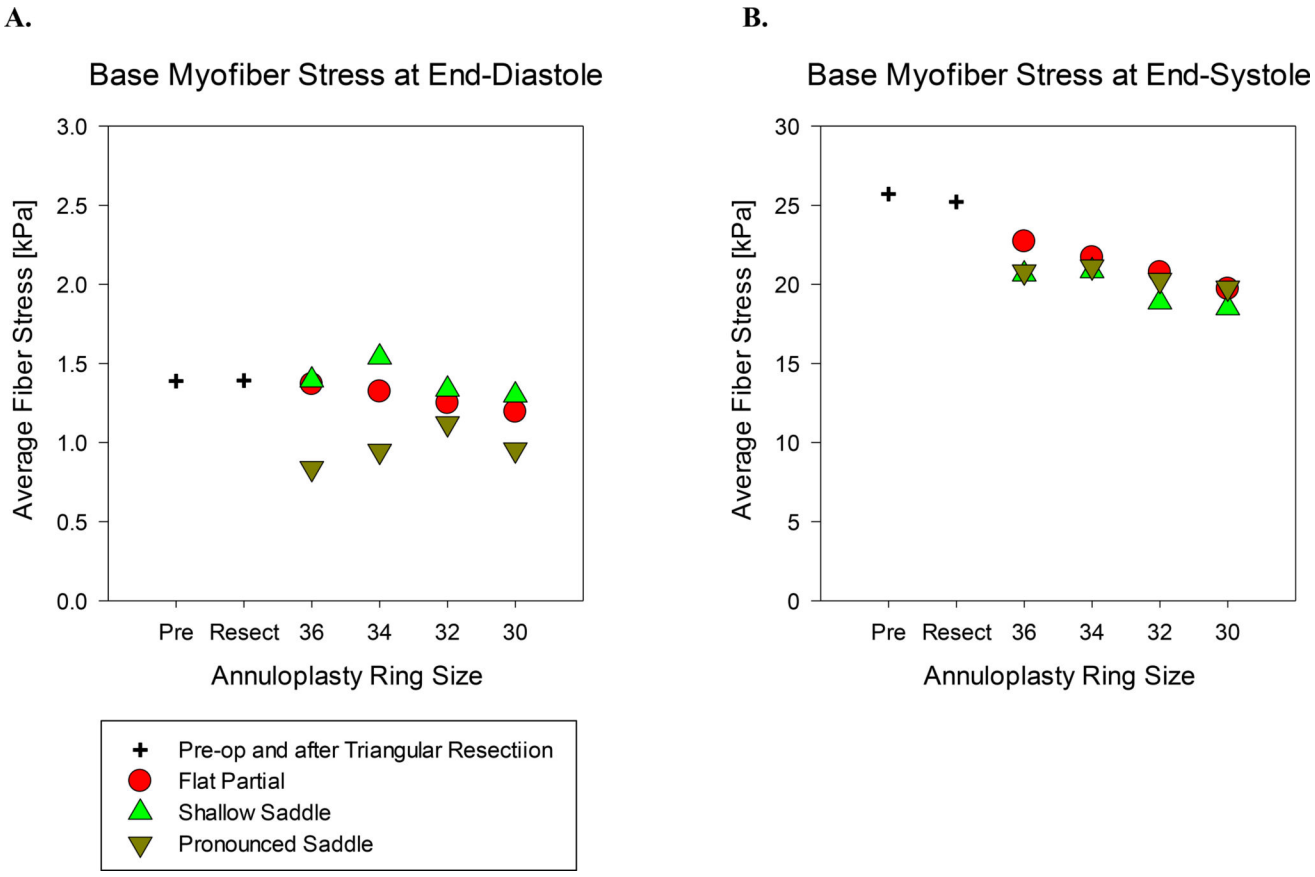

Figure 5.

Average myofiber stress in the LV base at end-diastole (**A**) and end-systole (**B**). Abbreviations are similar to Figure 2.

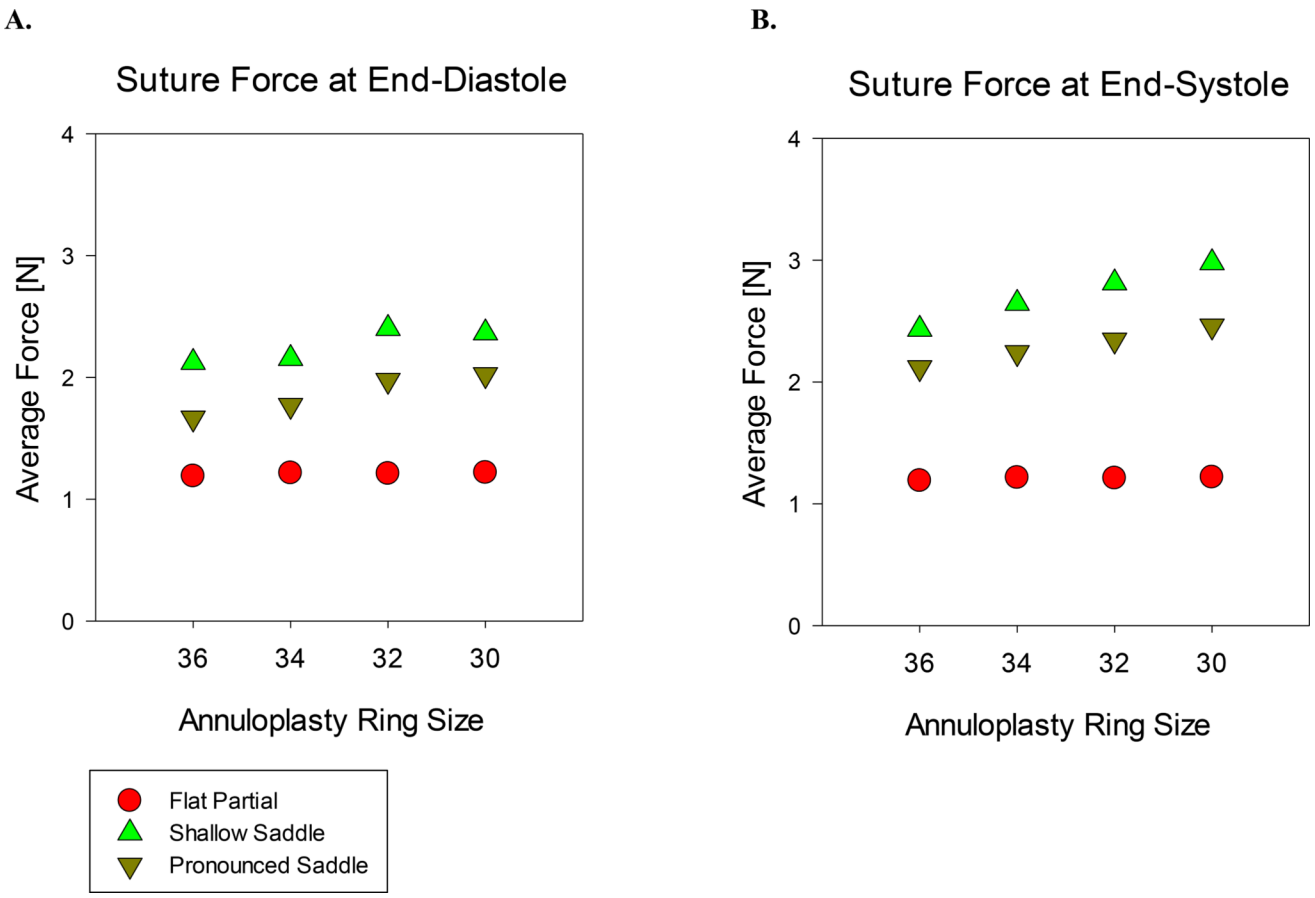

Figure 6.
Average suture force at end-diastole (**A**) and end-systole (**B**). 30, 32, 34 and 36 are annuloplasty device sizes.

Table 1

Mitral annuloplasty device properties

Device	Company	Style	Shape	Size of Sample
CG Future Band	Medtronic (Minneapolis, MN)	Partial	Flat band	36
Physio II Ring	Edwards Lifesciences (Irvine, CA)	Complete	Shallow saddle	24
Profile 3D Ring	Medtronic (Minneapolis, MN)	Complete	Pronounced saddle	32

Table 2

Mitral annuloplasty device sizes and their corresponding transverse diameters when modeled

Listed Size	Transverse Diameter (mm)
36	38.45
34	36.45
32	34.45
30	32.45